Measurement of the second-order Zeeman effect on the sodium clock transition in the weak-magnetic-field region using the scalar Aharonov-Bohm phase

Kazuya Numazaki, Hiromitsu Imai, and Atsuo Morinaga
Department of Physics, Faculty of Science and Technology, Tokyo University of Science, 2641 Yamazaki, Noda-shi, Chiba 278–8510, Japan
(Received 17 November 2009; published 30 March 2010)

The second-order Zeeman effect of the sodium clock transition in a weak magnetic field of less than 50 μT was measured as the scalar Aharonov-Bohm phase by two-photon stimulated Raman atom interferometry. The ac Stark effect of the Raman pulse was canceled out by adopting an appropriate intensity ratio of two photons in the Raman pulse. The Ramsey fringes for the pulse separation of 7 ms were obtained with a phase uncertainty of $\pi/200$ rad. The nondispersive feature of the scalar Aharonov-Bohm phase was clearly demonstrated through 18 fringes with constant amplitude. The Breit-Rabi formula of the sodium clock transition was verified to be $\Delta\nu = (0.222 \pm 0.003) \times 10^{12} \times B^{1.998\pm0.004}$ in a magnetic field of less than 50 μT.

DOI: 10.1103/PhysRevA.81.032124 PACS number(s): 03.65.Vf, 32.60.+i, 37.25.+k, 06.30.Ft

I. INTRODUCTION

The transitions between the $m = 0$ sublevels of the ground and excited states are used as the "clock transition" of frequency standards [1] or the "light-based beam splitter" of the Ramsey-type atom interferometer [2], because it has no first-order Zeeman frequency shift. However, the resonance frequencies of these transitions are still shifted by the second-order Zeeman effect even in a weak magnetic field. For precise measurements, this shift must be eliminated by magnetic shielding, as it is desirable to operate the interferometer at the smallest possible bias magnetic field [3]. However, a certain bias field strength is necessary to define a proper quantization axis and to prevent Majorana spin flips when the atoms enter the magnetically shielded region. In such a weak magnetic field region, this shift is usually estimated and corrected by the Breit-Rabi formula [4] with fundamental physical constants or experimental values. However, experimental verification of this formula will be indispensable. Up to now, the Breit-Rabi formula was tested usually in magnetic fields exceeding 100 μT (1 G) [5,6]. It was very difficult to measure the frequency shift of resonance transition at the strength of the usual bias magnetic field of less than 50 μT, because the magnitude of the shift becomes smaller than the width of the spectrum, which is determined by the width of the resonance pulse.

In 1959, Aharonov and Bohm predicted that the phase shifts in quantum mechanics when the time-dependent homogeneous scalar potential is applied during the interference region in the matter interferometer [7]. This is well known as the scalar Aharonov-Bohm shift and has been verified using neutral particles with magnetic moment in a magnetic field [8,9]. One of the authors (A.M.) and his colleagues have already demonstrated this shift due to the first-order Zeeman effect using the magnetic-field-sensitive transition of sodium atoms in the two-photon stimulated Raman atom interferometer [10]. The magnitude of the phase shift can increase when we apply a longer time of perturbation, even if the magnetic field is weak. Therefore, we aimed to utilize this shift to measure the second-order Zeeman effect of the sodium clock transition in the magnetic field region of less than 50 μT and attempted to verify the Breit-Rabi formula in the weak magnetic field region.

In this article, first we describe the principle of measurement of the second-order Zeeman effect as a scalar Aharonov-Bohm phase using a two-photon stimulated Raman interferometer. Next, we describe our experimental apparatus, procedure, and performance in detail. In particular, the ac Stark effect of Raman pulses was canceled out, because it is a disturbance to the measurement of the second-order Zeeman effect. Then, we show beautiful nondispersive interference fringes of the sodium clock transition as a function of the magnetic field strength. Finally, we confirmed that the Breit-Rabi formula of clock transitions holds in magnetic fields of less than 50 μT.

II. PRINCIPAL OF EXPERIMENT

The clock transitions between $m_F = 0$ and $m_F = 0$ hyperfine states are free from the Zeeman effect to the first order, and they are often called "magnetic-field-insensitive transitions." However, these transitions still show a second-order Zeeman effect. The frequency shift is calculated using second-order perturbation theory and is described by the well-known Breit-Rabi formula at the strength of the magnetic field B as

$$\Delta\nu = \frac{(g_J - g_I)^2 \mu_B^2}{2h^2 \Delta_{\mathrm{hfs}}} B^2 \equiv K B^2, \tag{1}$$

where g_J and g_I are fine structure and nuclear Lande g factors, μ_B is the Bohr magneton, h is Planck's constant, and Δ_{hfs} is the hyperfine splitting frequency.

A partial energy diagram of sodium atoms is shown in Fig. 1. For a sodium clock transition between the $^2S_{1/2}$, $F = 2$, $m_F = 0$ states and the $^2S_{1/2}$, $F = 1$, $m_F = 0$ states, the coefficient of the square of magnetic field K is 0.221 83 Hz/μT^2, as determined using their physical constants and experimental values [11]. Therefore, at 10 μT (0.1 G), where the degenerate of magnetic sublevels is resolved, the frequency shift is only 22 Hz. This shift is too small to compare with the spectrum width (1 kHz) of a typical Rabi pulse with a pulse width of 1 ms.

On the other hand, in quantum mechanics, the phase of the quantum, that is, a particle with charge q, magnetic moment μ, or polarizability α, is shifted by the temporal variation of the electromagnetic interaction, such as $q\phi$, μB, or αE^2, where ϕ,

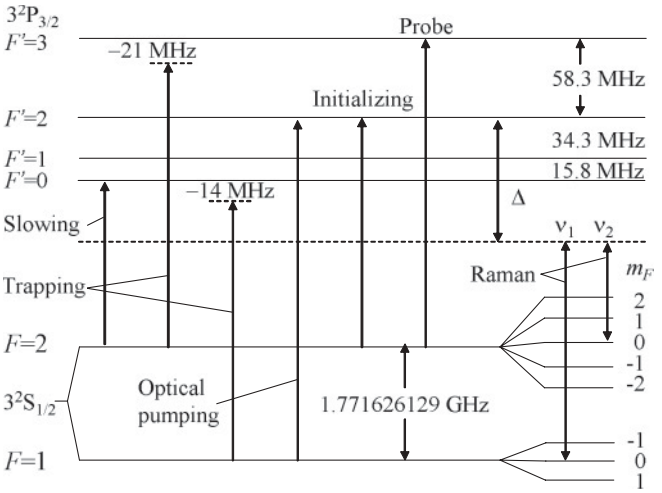

FIG. 1. Partial level scheme of sodium atoms and laser transitions for experiment. Δ, frequency of one photon detuning; ν_1 and ν_2, frequencies of two-photon stimulated Raman transition.

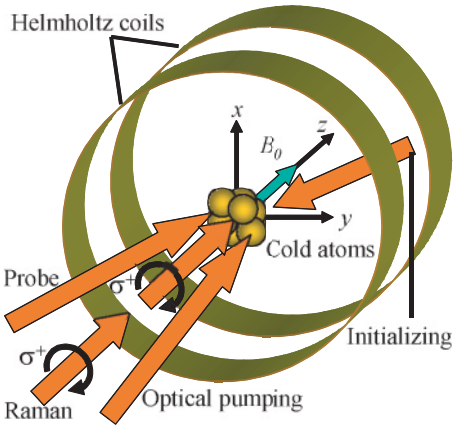

FIG. 2. (Color online) Schematic diagram for experiment. An ensemble of cold atoms in the quantization magnetic field B_0 along the z axis is irradiated by optical pumping, initializing, two σ^+-σ^+ circularly polarized two-photon stimulated Raman, and probe beams, sequentially.

B, and E are scalar potential, magnetic field, and electric field, respectively [12]. The phase shift is called the scalar Aharonov-Bohm shift. Similarly to the first-order Zeeman effect, which was observed in the magnetic-field-sensitive state with $m_F \neq 0$, the phase is shifted by the second-order Zeeman effect [13]. When the strength of a homogeneous magnetic field B is applied to atoms for the duration of perturbation T_B, the phase shift between the $F = 1, m_F = 0$ states and the $F = 2, m_F = 0$ states is given by

$$\Delta\varphi_{\mathrm{SAB}} = 2\pi K \int_0^{T_B} B(t)^2 dt. \tag{2}$$

This shift can be measured using a time-domain atom interferometer.

The time-domain atom interferometer composed of two ground hyperfine spin states of the sodium atom, $F = 1, m_F = 0$ and $F = 2, m_F = 0$ states, was produced by two excitations of cold atoms with circularly polarized copropagating two-photon stimulated Raman pulses separated by a time interval T [14]. The frequencies of the two-photon stimulated Raman pulse are ν_1, which is detuned by Δ far from the frequency of transition from the $^2S_{1/2}$, $F = 1, m_F = 0$ state to the $^2P_{3/2}$, $F' = 2$, $m_{F'} = 1$ state, and ν_2, which is detuned far from the transition from the $^2P_{3/2}$, $F' = 2$, $m_{F'} = 1$ state to the $^2S_{1/2}$, $F = 2, m_F = 0$ state, as shown in Fig. 1. The frequency difference between ν_1 and ν_2 is around 1.771 626 GHz, which corresponds to the frequency difference between the $F = 1$, $m_F = 0$ states and the $F = 2$, $m_F = 0$ states. Then it is free from the recoil momentum owing to the irradiation of two copropagating laser beams [10].

The quantization magnetic field B_0 is applied to the atoms in advance. The Raman pulses are radiated to an ensemble of cold atoms parallel to the direction of the quantization magnetic field, as shown in Fig. 2. Under this condition, the resonance frequency is shifted slightly by a second-order Zeeman effect of the quantization magnetic field. There is no phase shift in the Ramsey fringes, since B_0 is constant during T. When we change the strength of the magnetic field from B_0 to B with duration T_B ($<T$) rectangularly during the separation time T, the phase is shifted by

$$\Delta\varphi_{\mathrm{SAB}} = 2\pi K\left(B^2 - B_0^2\right)T_B. \tag{3}$$

Therefore, if we use a longer T_B, the phase shift for a small magnetic field difference can be measured.

III. EXPERIMENT

A. Laser setup

The laser setup was improved from that used in our previous studies [14,15]. Figure 3 shows our present laser setup. Two single-frequency ring dye (R6G) lasers were pumped by a 14-W multiline argon ion laser. One dye laser (DL1) produced about 1 W and the other (DL2) 0.5 W at a wavelength of 589 nm. The frequency of DL1 was stabilized to the isolated o-hyperfine component of the 15-2 band, P(38) line of

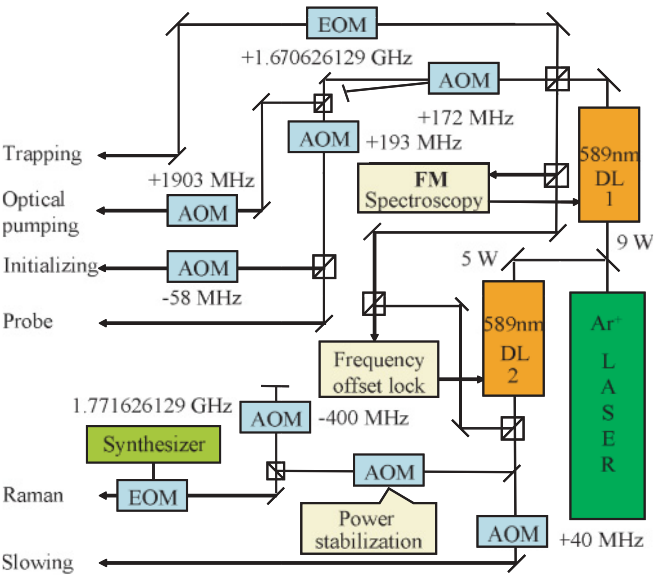

FIG. 3. (Color online) Experimental setup of lasers. DLs, dye lasers; AOMs, Acousto-optic modulators; EOMs, electro-optic modulators.

molecular iodine located at 467.6 MHz higher than the transition from the $F = 2$ to the $F' = 3$ state using FM saturation spectroscopy [15], and the frequency of DL2 was offset locked to the frequency of DL1. The outputs from DL1 were split, switched on and off, frequency-shifted using acousto-optic modulators (AOMs), and phase-modulated using an electro-optic modulator (EOM) as a trapping beam, an optical pumping beam, an initializing beam, and a probe beam, as shown in Fig. 1. One frequency of trapping beams was tuned 21 MHz lower than the transition from the $F = 2$ to the $F' = 3$ state and the other was tuned 14 MHz lower than the transition from the $F = 1$ to the $F' = 0$ state for dual-operated MOT [16]. The frequency of the optical pumping beam is the resonant frequency of the $F = 1$ to $F' = 2$ transition, and the frequency of the initializing beam is the resonant frequency between the $F = 2$ and the $F' = 2$ states. The frequency of the probe beam is the resonant frequency between the $F = 2$ and the $F' = 3$ states.

The outputs from DL2 were used as a Zeeman slowing beam and a Raman beam. The frequency of the Zeeman slowing beam was 110 MHz lower than that of the transition between the $F = 2$ and the $F' = 3$ states [17]. The ν_2 of the Raman beam was controlled to about 490 MHz below the resonance frequency from the $F = 2, m_F = 0$ to the $F' = 2$, $m_{F'} = 1$ states, and its power was stabilized within 1% using an AOM. The difference frequency between ν_1 and ν_2 and the intensity ratio of ν_1 to ν_2 were controlled by an EOM driven by a synthesizer and switched on and off by another AOM. This scheme has the superior feature that optical frequency jitter can be canceled out in the atom-laser interaction [18].

B. Experimental procedure

The sodium atomic beam was decelerated by a Zeeman slower and confined in the vacuum chamber using a dual-operated magneto-optical trap, a temporal dark trap, and polarization gradient cooling [19]. The number of trapped atoms was 10^9 with a peak density of 10^{11} particles/cm^3 and their temperature was about 200 μK.

The time sequence of measurement is shown in Fig. 4. At a few milliseconds after the release of atoms from the trap, a quantization magnetic field of about 10 μT was applied and all trapped atoms were optically pumped to the $F = 2$ state using the optical pumping beam for 100 μs, and the number of atoms was measured using a transmission of the probe beam. Subsequently, all atoms were initialized to the $F = 1$ state using the initializing beam for 100 μs. In order to construct a time-domain atom interferometer, two σ^+-σ^+ circularly polarized two-photon stimulated Raman pulses separated by time interval T were irradiated to the cold atoms parallel to the direction of the quantized magnetic field. The intensity ratio of ν_1 to ν_2 of the Raman pulse was regulated using the modulating rf power of the synthesizer. The pulse area of the Raman pulse was controlled to be $\pi/2$. Under a typical condition, the width of the Raman pulse τ was 11 μs and the intensity of the Raman pulse was 3.8 mW/cm^2. Upon the excitation of one resonant Raman pulse with a π pulse area, one third of the atoms in the $F = 1$ state are excited to the $F = 2, m_F = 0$ state. The separation time T between two Raman pulses was varied from 33 μs to 10 ms, which corresponds to a fringe cycle of 30 kHz to 100 Hz.

During the interval between two pulses, the strength of the magnetic field was changed promptly and returned to the original after the duration of T_B. Then the number of atoms in the $F = 2$ state was measured again using the probe beam, and the population probability in the $F = 2$ state was obtained. This sequence was repeated every 30 ms, and usually, 20 measurements were averaged. The experiment was performed as a function of the detuning frequency, the strength of the quantization magnetic field, or the time duration of T_B. The timing was controlled by a graphical program language (National Instruments, LabView).

C. Cancellation of ac Stark effect

To observe Ramsey fringes, we apply two $\pi/2$ Raman pulses, which are separated by a time interval T, on an ensemble of cold atoms. With equal-intensity two-photon Raman pulses, we observe Ramsey fringes with a fringe cycle of $1/(\tau + T)$ in the Rabi spectrum, as shown in Fig. 5. However, the Ramsey fringes are shifted depending on the intensity of the Raman pulses. First, the center frequency of the envelope is shifted by 16.3 kHz from the resonance frequency without perturbation, which is denoted by 0 kHz, and second,

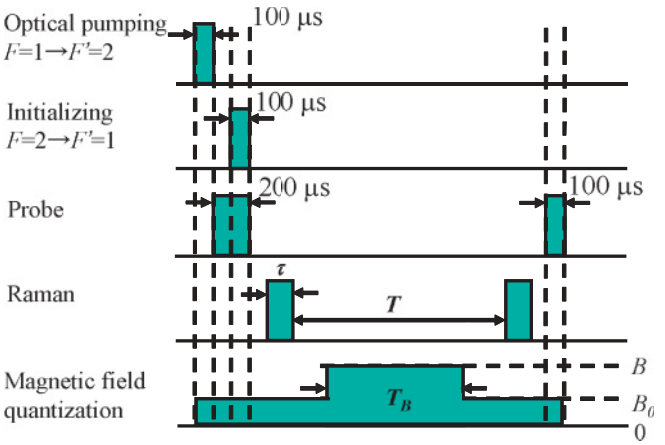

FIG. 4. (Color online) Timing diagram for measurement after release of ensemble of cold atoms from magneto-optical trap. τ, Raman pulse width; T, separation time between two Raman pulses; T_B, duration time of perturbed magnetic field.

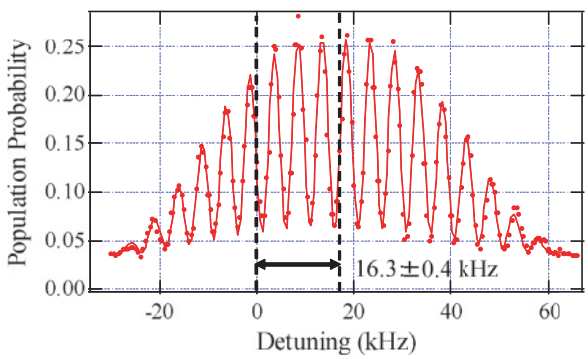

FIG. 5. (Color online) Ramsey fringes with equal-intensity two-photon Raman pulses. The pulse width of the Raman pulse was 20 μs and the separation between two Raman pulses was 180 μs. Resonance frequency and phase of fringes are shifted.

the phase of Ramsey fringes at the center frequency is shifted from 0 rad. The frequency shift of the envelope is the ac Stark frequency shift δ^{ac} and the phase shift is the scalar Aharonov-Bhom phase due to the time variation of the ac Stark potential, since the ac Stark potential disappears temporarily during T. The phase shift is $\Delta\varphi_{\mathrm{SAB}} = 2\pi\delta^{\mathrm{ac}}T$. These frequency and phase shifts must be removed to investigate the second-order Zeeman effect precisely.

In two-photon stimulated Raman transitions, the shifts are intrinsically related to the differential ac Stark shift caused by the imbalanced Raman beams, that is, $\delta^{\mathrm{ac}} = \Omega_e^{\mathrm{ac}} - \Omega_g^{\mathrm{ac}}$, where Ω_e^{ac} and Ω_g^{ac} are the frequency shifts of the excited and ground states, respectively, caused by the presence of the light fields [3,20]. As Ω^{ac} depends on the detuning frequency and intensity of the Raman beam, the shift can essentially be eliminated by properly adjusting the detuning and the intensity ratio of ν_1 to ν_2 in the Raman beam at a certain detuning frequency Δ. With the detuning of 0.49 GHz from the intermediate states, we adjusted the shifts by changing the intensity of the relevant Raman beam.

The two-photon Raman pulses were produced using an EOM driven at a frequency of around 1.771 626 GHz, where the carrier frequency and +1-order sideband frequency were used for the two photons. However, the EOM produced the −1-order sideband frequency with the same intensity as that of the +1-order sideband frequency. Therefore, the −1-order sideband frequency must also be taken into consideration for the calculation of shifts. The intensities of the carrier, the +1-order sideband, and the −1-order sideband are I_0, I_1, and $I_{-1} = I_1$, respectively. If the frequency difference between the F' state and the $F' = 2$ state is $\Delta_{F'}$,

$$\Omega_e^{\mathrm{ac}} \equiv \sum_{F'=1}^{3} \frac{|\langle F'|e\vec{r}|2\rangle|^2}{4\pi c\varepsilon_0\hbar^2}\left(\frac{I_1}{\Delta+\Delta_{F'}-\Delta_{\mathrm{hfs}}}+\frac{I_0}{\Delta+\Delta_{F'}}+\frac{I_1}{\Delta+\Delta_{F'}+\Delta_{\mathrm{hfs}}}\right), \tag{4}$$

and

$$\Omega_g^{\mathrm{ac}} \equiv \sum_{F'=1}^{2} \frac{|\langle F'|e\vec{r}|1\rangle|^2}{4\pi c\varepsilon_0\hbar^2}\left(\frac{I_1}{\Delta+\Delta_{F'}}+\frac{I_0}{\Delta+\Delta_{F'}+\Delta_{\mathrm{hfs}}}+\frac{I_1}{\Delta+\Delta_{F'}+2\Delta_{\mathrm{hfs}}}\right). \tag{5}$$

From $\Omega_e^{\mathrm{ac}} = \Omega_g^{\mathrm{ac}}$, the intensity ratio of the carrier to the +1-order sideband is calculated to be 1.95 for $\Delta = 490$ MHz, independent of the total intensity of the Raman beam. In the experiment, the intensity ratio was changed for a total power of 1.3 and 3.8 mW/cm^2 and the center frequency of the Rabi spectrum was measured, as shown in Fig. 6. The pulse width for the $\pi/2$ pulse was 11 and 34 μs, respectively. The center frequency changed with intensity ratio according to the fitted solid curve and two solid curves were intersected at 1.94 ± 0.02, which is in good agreement with the calculation.

Figure 7 shows the Ramsey fringes observed at an intensity ratio of 1.98 for different separation times T as a function of detuning frequency. It should be noted that the population probabilities are maximum at the center frequency, which means there is no phase shift.

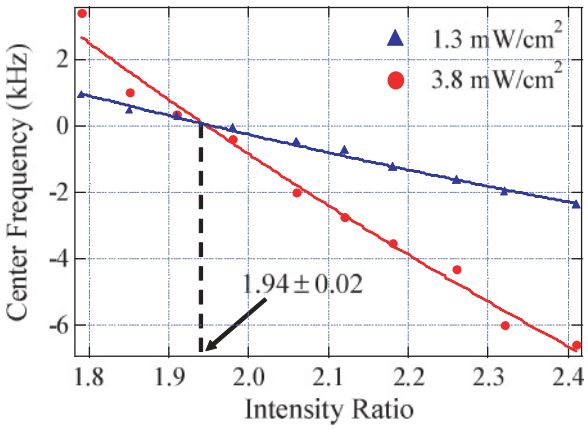

FIG. 6. (Color online) ac Stark frequency shifts versus intensity ratio of the two frequencies of Raman beam for different total laser intensities of 1.3 and 3.8 mW/cm^2. Two solid curves fitted to the experimental values cross at an intensity ratio of 1.94.

D. Amplitude of Ramsey fringes

Although the ensemble of cold sodium atoms was 200 μK, it was expanded to about 4 mm at 10 ms after release. As a result, the amplitude of Ramsey fringes decreased as separation time increased. The amplitude of the fringes was 0.15 at $T = 0.1$ ms, which corresponds to the almost complete excitation, as shown in Fig. 8. However, the amplitude was reduced to 0.123 at $T = 2$ ms and 0.033 at $T = 7$ ms, while the visibility of the fringes was reduced to 0.65 from 0.72 at $T = 2$ ms. The uncertainty of the phase measurement at $T = 7$ ms was 0.016. Therefore, we can measure the phase with a resolution of $\pi/200$ rad. The center frequency of each Ramsey fringe was slightly shifted, because of the second-order Zeeman effect depending on the strength of the weak quantization magnetic field and the uncompensated ac Stark frequency shift.

E. Magnetic field

The magnetic field strength was measured using the Zeeman frequency shift of the magnetic-field-sensitive transition. In advance, the magnetic field at the trap region

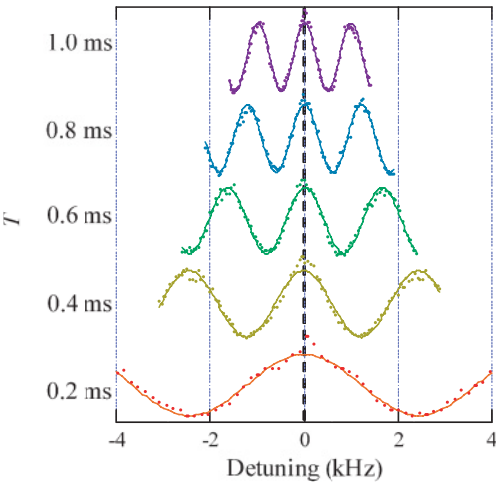

FIG. 7. (Color online) Ramsey fringes observed with cancellation of ac Stark frequency shift for various separation times T less than 1 ms. All center frequencies are coincident.

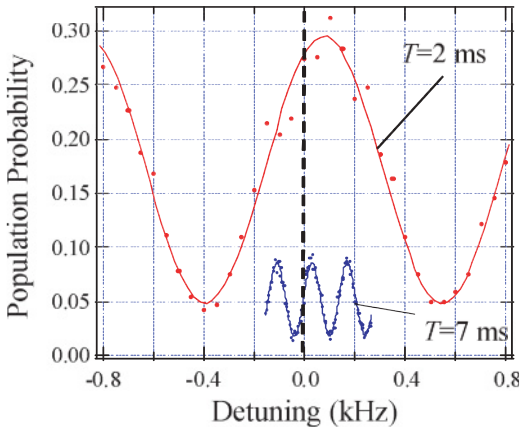

FIG. 8. (Color online) Ramsey fringes observed for long separation time $T = 2$ and 7 ms. Their visibilities are 0.72 and 0.65, respectively. There are still small frequency shifts of less than 100 Hz which occur from the second-order Zeeman frequency shift and residual ac Stark frequency shift.

was compensated less than 0.5 μT using three perpendicular Helmholtz coils. First, we confirmed the parallelism between the directions of the quantization magnetic field and the Raman beam by observing the spectra of three components: $m_{F=1} = 1$ to $m_{F=2} = 1$, $m_{F=1} = 0$ to $m_{F=2} = 0$, and $m_{F=1} = -1$ to $m_{F=2} = -1$, as shown in Fig. 9. There is no other peak which comes from the component of the magnetic field perpendicular to the direction of the Raman beam. When the width of the Raman pulse was 20 μs, the width of spectrum was 51.5 kHz, which was almost in the Fourier transform regime. The magnetic field strength was determined from the frequency separations between these spectra. The uncertainty of the field strength was 0.2%.

The shape of the magnetic field at rise-up or fall-off was inferred from the frequency shift when the Raman pulse with a pulse width of 20 μs was irradiated as a function of time. The data fitted an exponential curve well, with a relaxation time of about 30 μs for both. Therefore, the shape of the magnetic field was taken into consideration to obtain the scalar Aharonov-Bohm phase. The correction was estimated to be 0.4% at 50 μT for a pulse with a duration of 3 ms.

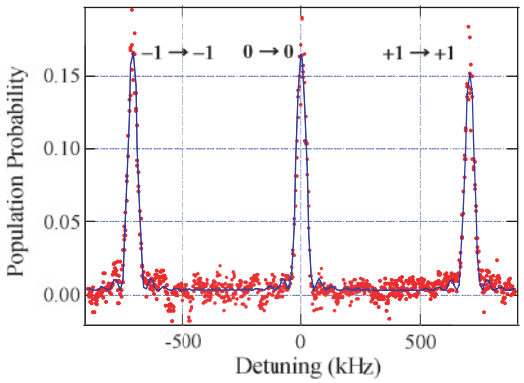

FIG. 9. (Color online) Zeeman splitting of sodium atoms excited by σ^+-σ^+ circularly polarized two-photon Raman pulse with a pulse width of 20 μs under a magnetic field of 50 μT. Figures denote $m_{F=1} \rightarrow m_{F=2}$.

IV. RESULTS AND DISCUSSION

A. Nondispersive fringes

The de Broglie wavelength of atoms with a thermal velocity distribution extends to the size of the wavelength, even if an ensemble of atoms is cooled to less than 1 mK. The atomic cloud within 10 ms after release from the trap maintains a temperature of 200 μK. The most probable velocity is 0.38 m/s and the velocity spread is 0.43 m/s. Then, the mean de Broglie wavelength is 46 nm and the coherent length is 16 nm. Therefore, interference fringes caused by the phase shift depending on the velocity of each particle disappear for phase shifts of more than one fringe, as shown in the spatial atom interferometer (for example, [21]). On the contrary, the essential feature of the scalar Aharonov-Bohm effect is nondispersivity, which is independent of the particle velocity [7]. The situation is realized if particles move in a force-free space; that is, the time-dependent potential must be uniform in the space where the particles travel under the potential. In neutron experiments, the magnetic field of the solenoid is only turned on and off when the wave function of the neutron is fully enclosed in the solenoid [8]. We discuss here the present experimental situation in detail. The cold sodium atoms are in the vicinity of the center of the Helmholtz coil, which is composed of two circular coils with a radius of 5.5 cm and the distance between them is 8 cm. The cold sodium atoms move 4 mm on average during 10 ms after release, but they still remain in the magnetic field. However, the calculation of the magnetic field predicts that the magnetic field has a gradient of at most 10% of the field strength within 5 mm from the center. This variation of the magnetic field changes the second-order Zeeman energy by 20%, which is 10^{-4} of the kinetic energy of cold sodium atoms with a temperature of 200 μK. Then it is estimated that the velocity of cold atoms changes by a ratio of 10^{-4}. This velocity dispersion due to the gradients of the second-order Zeeman effects will be negligible for a phase shift of less than 1000 fringes.

In order to examine the nondispersivity under the present conditions, we measured the population probability at a resonance frequency as a function of the magnetic field strength, as shown in Fig. 10. The T_B was 5 ms. The magnetic field strength changed from $B_0 = 9$ μT to $B = 130$ μT. The

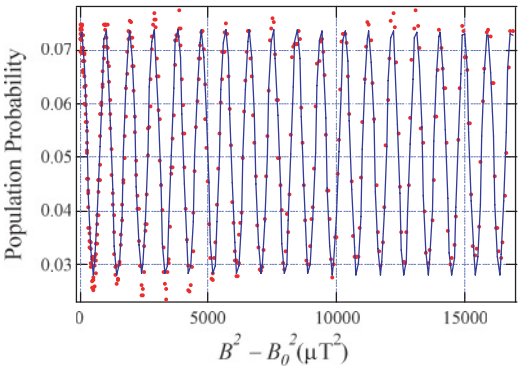

FIG. 10. (Color online) Interference fringes as a function of the square of the magnetic field B^2 with a duration of 5 ms. The fact that the amplitude of fringes is almost constant through 18 fringes shows the nondispersivity of the scalar Aharonov-Bohm phase.

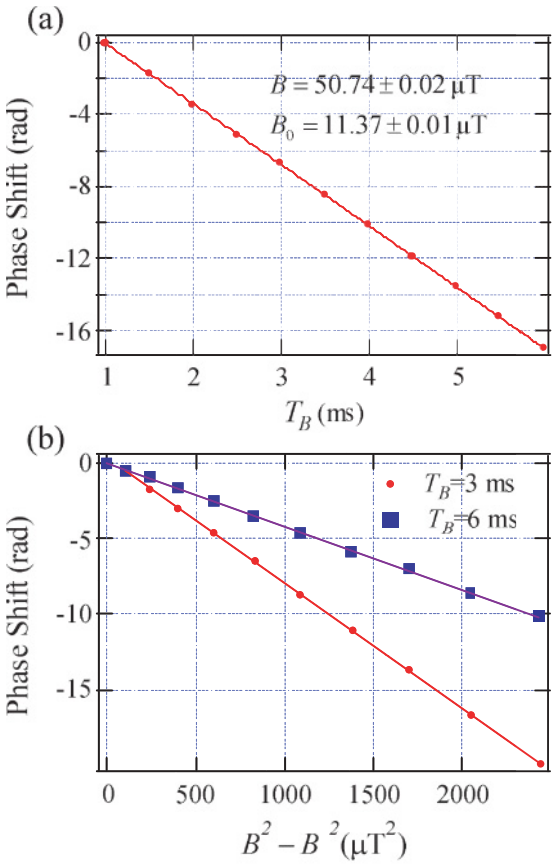

FIG. 11. (Color online) (a) Dependency of the phase shift on perturbation time T_B under the constant perturbed magnetic field B. (b) Dependency of the phase shift on the square of the magnetic field B^2 for durations of $T_B = 3$ and 6 ms.

horizontal axis is given as B^2-B_0^2. The population probability was fitted well by a cosine curve. We can see the 18 fringes with almost the same amplitude in the figure, so that nondispersivity of the scalar Aharonov-Bohm shift was confirmed using the second-order Zeeman effect.

B. Second-order Zeeman effect

In order to verify that the Zeeman effect on the clock transition is given by Eq. (3), first of all we measured the phase shift of Ramsey fringes as a function of T_B from 1 to 6 ms under the magnetic fields of $B_0 = 11.37 \pm 0.01$ μT and $B = 50.74 \pm 0.02$ μT. The results are shown in Fig. 11(a). The data were fitted well by a function of $T_B^{1.02\pm0.02}$, so it is confirmed that the phase is a linear function of T_B.

Next, the phase shifts were measured as a function of B from $B_0 = 11$ to 50 μT for durations of $T_B = 3$ and 6 ms. The results are shown in Fig. 11(b), where the horizontal axis is given as B^2-B_0^2. Both results show that the phases are shifted along straight lines and these data were well fitted by

$$\Delta\varphi_{\mathrm{SAB}} = 2\pi \times (0.222 \pm 0.003) \times 10^{12} \times \left(B^{1.998\pm0.004} - B_0^2\right) T_B, \quad (6)$$

where the units of B and B_0 are T and T_B is s. The obtained index shows the quadratic feature of the Zeeman effect on the magnetic field strength. By comparison with Eq. (3), the coefficient K is found to be 0.222 ± 0.003 Hz/μT^2, which is in good agreement with the coefficient of the Breit-Rabi formula of the sodium clock transition calculated with the fundamental physical constants and experimental values. Therefore, we verified the validity of the Breit-Rabi formula of the clock transition in a magnetic field of less than 50 μT.

V. CONCLUSION

The second-order Zeeman effect of the sodium clock transition in a weak magnetic field of less than 50 μT was investigated using the scalar Aharonov-Bohm phase in a time-domain atom interferometry. The time-domain atom interferometer was composed of two two-photon stimulated Raman pulses separated by a few milliseconds, which were radiated to an ensemble of cold sodium atoms. The ac Stark effect of the Raman pulse was canceled out by adopting an appropriate intensity ratio of two photons in the Raman pulse, so that the frequency and phase shifts at the resonance were coincident not depending on the total intensity of Raman pulses. For the pulse separation of 7 ms, the Ramsey fringes were obtained with a phase uncertainty of $\pi/200$ rad, when the temperature of cold atoms was 200 μK. The time-dependent magnetic field was applied to sodium atoms during two Raman pulses. The nondispersive feature of the scalar Aharonov-Bohm phase was clearly demonstrated through 18 fringes with constant amplitude. Finally, it was verified that the Breit-Rabi formula of the clock transition of sodium atoms is applicable in a magnetic field of less than 50 μT.

ACKNOWLEDGMENTS

The authors thank A. Takahashi for his discussion on the scalar Aharonov-Bohm shift due to the second-order Zeeman effect.

[1] R. Wynands and S. Weyers, Metrologia **42**, S64 (2005).
[2] M. Kasevich and S. Chu, Phys. Rev. Lett. **67**, 181 (1991).
[3] A. Peters, K. Y. Chung, and S. Chu, Metrologia **38**, 25 (2001).
[4] G. Breit and I. I. Rabi, Phys. Rev. **38**, 2082 (1931).
[5] S. A. Webster, P. Taylor, M. Roberts, G. P. Barwood, and P. Gill, Phys. Rev. A **65**, 052501 (2002).
[6] R-B. Li, L. Zhou, J. Wang, and M.-S. Zhan, Opt. Commun. **282**, 1340 (2009)
[7] Y. Aharonov and D. Bohm, Phys. Rev. **115**, 485 (1959).
[8] B. E. Allman, A. Cimmino, A. G. Klein, G. I. Opat, H. Kaiser, and S. A. Werner, Phys. Rev. Lett. **68**, 2409 (1992).
[9] S. Nic Chormaic, C. Miniatura, O. Gorceix, B. Viaris de Lesengo, J. Robert, S. Feron, V. Lorent, J. Reinhardt, J. Baudon, and K. Rubin, Phys. Rev. Lett. **72**, 1 (1994).
[10] K. Shinohara, T. Aoki, and A. Morinaga, Phys. Rev. A **66**, 042106 (2002).

[11] D. A. Steck, Sodium D Line Data (2008), http://steck.us/alkalidata.
[12] J. H. Müller, D. Bettermann, V. Rieger, K. Sengstock, U. Sterr, and W. Ertmer, Appl. Phys. B **60**, 199 (1995).
[13] A. Takahashi, H. Imai, K. Numazaki, and A. Morinaga, Phys. Rev. A **80**, 050102(R) (2009).
[14] H. Imai, Y. Otsubo, and A. Morinaga, Phys. Rev. A **76**, 012116 (2007).
[15] S. Watanabe, Y. Aizawa, and A. Morinaga, Jpn. J. Appl. Phys. **42**, 1462 (2003).
[16] H. Tanaka, H. Imai, K. Furuta, Y. Kato, S. Tashiro, M. Abe, R. Tajima, and A. Morinaga, Jpn. J. Appl. Phys. **46**, L492 (2007).
[17] V. S. Bagnato, C. Salomon, E. Marega Jr., and S. C. Zilio, J. Opt. Soc. Am. B **8**, 497 (1991).
[18] M. Kasevich and S. Chu, Appl. Phys. B **54**, 321 (1992).
[19] K. Matsui, H. Imai, H. Yamaoka, R. Makabe, K. Furuta, and A. Morinaga, Appl. Phys. Express **2**, 032301 (2009).
[20] D. S. Weiss, B. C. Young, and S. Chu, Appl. Phys. B **59**, 217 (1994).
[21] A. Morinaga, M. Nakamura, T. Kurosu, and N. Ito, Phys. Rev. A **54**, R21 (1996).